Astron. Astrophys. 322, 477–488 (1997)

ASTRONOMY
AND
ASTROPHYSICS

A study of the evolution of radio pulsars through improved population synthesis

J.W. Hartman[1], **D. Bhattacharya**[2], **R. Wijers**[3], **and F. Verbunt**[1]

[1] Astronomical Institute, Utrecht University, P.O.Box 80000, 3508 TA Utrecht, The Netherlands
[2] Raman Research Institute, 560 080 Bangalore, India
[3] Institute of Astronomy, Madingley Road, Cambridge 0HA CB3, UK

Received 9 May 1996 / Accepted 1 October 1996

Abstract. We simulate the birth and evolution of radio pulsars throughout the Galaxy and their observation in a region around the Sun, using recently derived models for the velocity distribution of neutron stars and for the galactic distribution of free electrons. We confirm our previous result that the properties of the pulsar population are best described by models in which the magnetic field does not decay significantly during the pulsar lifetime. The small number of young pulsars at large distance to the Galactic Plane suggests that many pulsars are born with small velocities. We derive a birth rate of radio pulsars near the Sun of $2.3\,\mathrm{kpc}^{-2}\,\mathrm{Myr}^{-1}$, and argue that this rate can be sustained by stars with mass M $>$ 10 Msun, in OB-associations.

Key words: stars: neutron – pulsars: general

1. Introduction

The evolution of the properties of single radio pulsars cannot be measured directly. It may be derived however from a study of the population of pulsars. Two powerful techniques that have been used to do so are pulsar-current analysis and population synthesis.

In pulsar-current analysis, one uses adjacent fields in the period - period-derivative plane or equivalently in the period - magnetic-field plane to constrain the evolution of pulsars from one field to another, by demanding continuity (Phinney & Blandford 1981, Deshpande et al. 1995). A major advantage of this method is that, in principle at least, it is model-independent. However, pulsars in adjacent fields in the P-$\dot{P}$ plane may have rather different detection probabilities, because of the important role of selection effects in the detection of radio pulsars. The necessity to model this removes much of the advantage of current studies above the other method, population synthesis (Lorimer et al. 1993).

Send offprint requests to: F. Verbunt, verbunt@fys.ruu.nl

In population synthesis one assumes distributions for the initial pulsar properties, and laws governing their evolution, to simulate a population of radio pulsars. When comparing this simulated population with the observed one, it is necessary to model the selection effects in some detail (Narayan & Ostriker 1990). In an earlier study we modelled the population of radio pulsars and its observation in four major surveys, and obtained the (to us, at least) surprising result that models in which the magnetic field decays little or not at all during the active life time of a radio pulsar give the best description of the observations (Bhattacharya et al. 1992, henceforth Paper I). For reviews on recent developments in the understanding of magnetic-field decay of radio pulsars see e.g. Verbunt (1994) and Bhattacharya (1995).

We limited our calculations in Paper I to pulsars in the surroundings of the Sun, with distances projected on the Galactic Plane of less than 3 kpc. In this region, the birth rate of radio pulsars was assumed to depend only on the distance z to the Galactic Plane, and the motion of pulsars in the galactic potential was described in the z-direction only (see also Hartman & Verbunt 1995).

Thus, our calculations did not take into account the effects of a gradient in the birthrate in the Galaxy, and the importance of net drifts in the positions of pulsars as they age. It is the goal of this study to remedy this, by calculating pulsar orbits throughout the whole Galaxy. In doing so we will also use the improved information that has become available since Paper I was written, on the distribution of electrons in our Galaxy – i.e. on the relation between dispersion measure DM and the distance of a pulsar – and on the velocity distribution of newly born neutron stars. The change of distance scale has induced us to also allow the assumed luminosity law to vary between model computations.

In Sect. 2 we describe the changes made in our code for our new model calculations. Because we want to understand separately the consequences of the use of updated electron density and velocity distributions, and the effects of the galactic drift of pulsars, we describe in Sect. 3 calculations done in the environs

of the Sun with the updated distributions, before describing in Sect. 4 the calculations in which pulsars are assumed to be born throughout the Galaxy, even though their observation is limited to the solar surroundings. Our conclusions are discussed in Sect. 5.

2. The population synthesis technique

In this paper we use the same pulsar population synthesis technique as described in Paper I, and the reader is referred to that paper for details. Briefly, we choose distributions for the positions, velocities and magnetic fields for newly born pulsars. We use a Monte Carlo method to pick a pulsar from these distributions and to assign an age to it. We calculate the evolution of its period and magnetic field in time, and its orbit in the galactic potential. We check whether the pulsar is still above the death-line (below which a radio pulsar is not detectable), and whether the pulsar is beamed towards us. From the period and period derivative we calculate a model luminosity. We choose the actual luminosity from a distribution of luminosities around this model luminosity. From the position we calculate the dispersion measure and scattering time. Finally we check whether the pulsar meets the detection criteria of one of four major pulsar surveys. This procedure is repeated until we have a large enough sample of simulated pulsars. The properties of this sample are compared by means of Kolmogorov-Smirnov tests with the properties of those real pulsars that meet the above-mentioned detection criteria.

In the remainder of this section we detail the changes in our synthesis technique with respect to Paper I.

2.1. Dispersion measure

Taylor and Cordes (1993) have modelled the electron density distribution in our Galaxy in detail, taking into account the presence of spiral arms, and the finite scale height of the electron distribution as derived from the dispersion measures of radio pulsars in globular clusters (see also Reynolds 1989, Bhattacharya & Verbunt 1991). We use the code provided by them to calculate the dispersion measure and scattering time. To save computing time during the runs, we compute the values on a grid and use second-order interpolation on this grid during our simulations. We use a Cartesian coordinate system in which the x-y plane is the Galactic Plane with y pointing towards the Galactic Center, and z the distance to the Galactic Plane. The grid is centered on the Sun and extends from -4 to +4 kpc with 0.1 kpc spacing in x and y. The z grid consists of 35 mesh points between 0 and 3.5 kpc with spacing increasing with z. Values at greater z can be found by extrapolation, since the electron density above 3.5 kpc is very small. The differences between interpolated values and those computed directly are small enough to have no influence on our results. The median difference for pulsar positions chosen randomly within the grid but restricted to $|z| < 1$ kpc is 0.02%, and 99% of all DM values are accurate to better than 1%. If we do not restrict the positions to low z the differences are even less, but since most detected pulsars are at low z that would not be a realistic representation. Near the Gum Nebula there are some small regions with differences up to 20%, due to the fact that the Gum Nebula has a scale length comparable to our grid size, but the overall effect of this on our simulations is again negligible. The median difference between the full model and our interpolation in scattering time is 0.07%, and 99% of the scattering times are accurate to better than 4%.

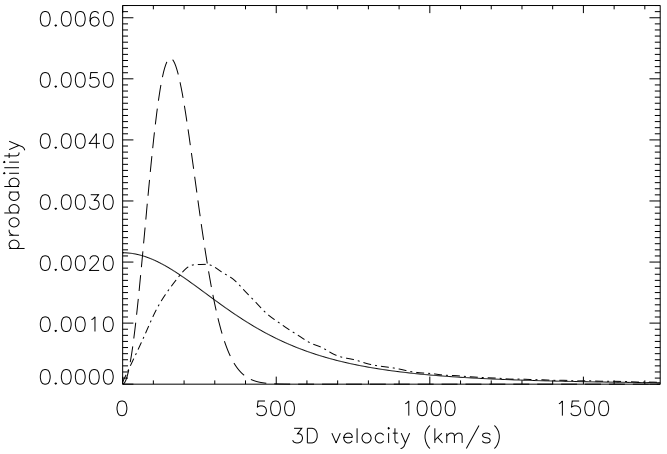

Fig. 1. The velocity distribution of young neutron stars as determined by Lyne & Lorimer (1994) (dashed-dotted line) and according to Phinney-Paczyński (solid line, see Eq. 1), normalized to unity. The dashed line represents a 3 dimensional Maxwellian velocity distribution that follows from the 1 dimensional Gaussian distribution with a width of 110 km s^{-1} that we used in Paper I.

2.2. The velocity distribution

Due to the change in derived distances with the implementation of the new model for the electron density distribution, as well as due to new measurements, a new description of neutron star velocities has become necessary. Lyne & Lorimer (1994) have derived a 3-dimensional velocity distribution which we model using a smooth fit to a table of numbers representing the differential distribution, kindly supplied to us by D. Lorimer. The distribution peaks at about 250 km/s and extends to velocities above 1000 km/s.

It has been argued by Hansen & Phinney (priv. comm.) that the 3-dimensional velocity distribution of radio pulsars is not strongly constrained at low velocities, and could well peak at small velocities, e.g. according to an equation first given by Paczyński (1990):

$$p(u)\mathrm{d}u = \frac{4}{\pi}\frac{\mathrm{d}u}{(1+u^2)^2}, u = \frac{v_\mathrm{i}}{\sigma_v} \quad (1)$$

with $\sigma_v \simeq 600$ km/s. These two distributions are shown in Fig. 1.

2.3. The luminosity distribution

With different distances, different luminosities are derived from the observed fluxes. In our calculations, model luminosities are

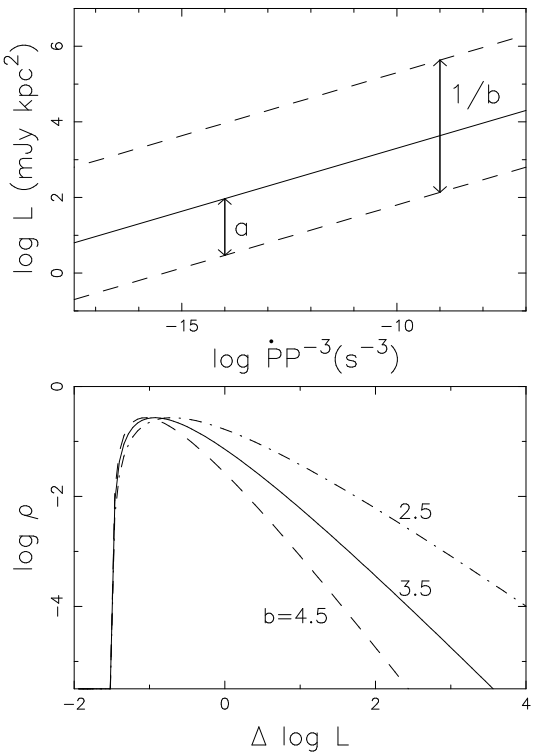

Fig. 2. Top panel: the model luminosity L_m as a function of P and $\dot{P}$ according to Eq. 2 (solid line). The two dashed lines roughly delineate the range of the pulsar luminosities around L_m, and its dependence on a and b (see Eq. 2). Bottom panel: the shape of the distribution ρ_L of the pulsar luminosities around L_m, for a = 1.5 and for different values of b.

derived in two steps from the periods and period derivatives. First, the luminosity L_m is derived from P and $\dot{P}$ with use of the luminosity law according to Prószyński & Przybicień (1984)

$$\log L_m = 6.635 + \frac{1}{3}\log\frac{\dot{P}}{P^3} \tag{2}$$

The second step consists in the choice of a deviation $\Delta\log L \equiv \log L_{400} - \log L_m$ from L_m of the actual model luminosity L_{400}. We follow Narayan & Ostriker (1990) in writing the distribution of these deviations as

$$\begin{aligned}\rho_L(\lambda) &= 0.5\lambda^2 e^{-\lambda} \quad \text{for } \lambda \geq 0 \\ &= 0 \qquad\qquad\quad \text{for } \lambda < 0\end{aligned} \tag{3}$$

where

$$\lambda \equiv b(\log\frac{L_{400}}{L_m} + a)$$

The lower limit to the luminosity and the width of the luminosity distribution at given L_m are determined by a and b respectively, as illustrated in Fig. 2.

In Paper I, we tested the simulated luminosity distribution against the observed one, but not the dependence of the luminosity on $\dot{P}P^{-3}$. In test calculations we find that flattening the slope of the luminosity law (Eq. 2) leads to a simulated luminosity distribution with a dependence of the luminosity on $\dot{P}P^{-3}$ which is not compatible with the observed distribution. In this paper, we therefore allow the parameters a and b to vary, but keep Eq. 2 fixed.

2.4. Pulsars in the whole galaxy

In our simulations we choose the initial galactocentric radius of a pulsar R_i either from an exponential distribution

$$p(R_\mathrm{i})\mathrm{d}R_\mathrm{i} = \frac{1}{R_\mathrm{w}}\exp(-\frac{R_\mathrm{i}}{R_\mathrm{w}})\mathrm{d}R_\mathrm{i} \tag{4}$$

or from a Gaussian distribution

$$p(R_\mathrm{i})\mathrm{d}R_\mathrm{i} = \frac{1}{\sqrt{2\pi R_\mathrm{w}^2}}\exp(-(R_\mathrm{i}-R_\mathrm{off})^2/2R_\mathrm{w}^2)\mathrm{d}R_\mathrm{i} \tag{5}$$

where $R_\mathrm{i} > 0$ and where R_w is the scale length of the distribution, and R_off the offset from the maximum of the Gaussian distribution to the Galactic Center (see e.g. Johnston 1994).

The initial z-distribution is as in Paper I, and the initial ϕ-distribution is uniform between 0 and 2π.

To integrate the pulsar orbits in the galactic potential we follow Lorimer et al. (1993) and adopt the modification by Kuijken & Gilmore (1989) of the Carlberg & Innanen (1987) fit of the Galactic Potential. This model consists of three components: a disk + halo component Ψ_{dh}, a bulge component Ψ_b and a nucleus component Ψ_n. The total galactic potential can then be written as:

$$\Psi = \Psi_{dh}(R,z) + \Psi_b(R) + \Psi_n(R) \tag{6}$$

where

$$\Psi_{dh}(R,z) = \frac{-GM_{dh}}{[(a_G + \sum_{i=1}^{3}\beta_i\sqrt{z^2+h_i^2})^2 + b_{dh}^2 + R^2]^{1/2}} \tag{7}$$

where the summation models the contribution of dark matter and of the old and young disc. Further, we have

$$\Psi_{b,n}(R) = \frac{-GM_{b,n}}{\sqrt{b_{b,n}^2 + R^2}} \tag{8}$$

The constants that we use in eqs. 7, 8 are listed in Table 1.

The orbit integration is done with the 4th order Runge Kutta method with variable time step(Press et al. 1992), on the variables R, $\dot{R}$, z, $\dot{z}$, and ϕ. We use conservation of angular momentum to calculate v_ϕ as a function of R: $j = Rv_\phi$.

2.5. The real pulsar sample

The properties of the real pulsars to be compared with our synthesized population are taken from the last published version of the Princeton pulsar catalog (Taylor et al. 1993). In most models, we include only pulsars whose distance projected on the Galactic Plane, d_proj, is less than 4 kpc. In this way we keep

Table 1. The parameters for the Galactic Potential as given by Kuijken & Gilmore (1989)

parameter	disk+halo	nucleus	bulge
Mass ($M_\odot$)	1.45 10^{11}	9.3 10^9	1.0 10^{10}
β_1	0.4		
β_2	0.5		
β_3	0.1		
h_1(kpc)	0.325		
h_2(kpc)	0.090		
h_3(kpc)	0.125		
a_G(kpc)	2.4		
$b_{dh,n,b}$(kpc)	5.5	0.25	1.5

the number of pulsars in the comparison sample sufficiently large for statistical accuracy, while avoiding the larger uncertainties in dispersion measure at larger distances. The surveys we use to compare our simulations with are: the Jodrell Bank survey (Davies et al. 1972), the U Mass Arecibo survey (Hulse & Taylor 1974), the Second Molonglo survey (Manchester et al. 1978) and the U Mass NRAO survey (Damashek et al. 1978). This leaves us for most models with a sample consisting of 129 pulsars.

2.6. Test quantities and confidence levels of the fits

To quantify the merit of a model, we perform Kolmogorov-Smirnov tests to compare the distributions in the real pulsar sample and the simulation of four quantities: P, B, $DM \sin b$ and L_{400}. The figure of merit used for the model is the product of the four K-S probabilities, $Q_4^{\rm real}$. To get a confidence level for accepting or rejecting the fit, we need to calculate the probability distribution function of Q_4 for a perfect model, which does not follow simply from K-S theory. Then we compute the probability, $P_{\rm fit}$, that the value of Q_4 for a perfect model be poorer than $Q_4^{\rm real}$:

$$P_{\rm fit} \equiv \int_0^{Q_4^{\rm real}} f(Q_4){\rm d}Q_4 = F(Q_4^{\rm real}) \qquad (9)$$

$f(Q_4)$ can be approximated with a bootstrap technique as follows: our simulations give samples of $N_{\rm sim}$ simulated pulsars for each model. We create two such simulated samples with the same model but a different random seed. One of these plays the role of 'model', the other that of 'nature', which means that the 'model' is a statistically perfect fit to 'nature' by construction. From 'nature' we now draw a sample of $N_{\rm real}$ pulsars ($N_{\rm real}$ is the size of the real pulsar sample, usually 129 in this paper) and compute its fit merit Q_4 with the 'model' simulation. By repeating this bootstrap procedure $N_{\rm boot}$ times we construct the distribution function $f_{\rm boot}(Q_4)$ of merit values. The theory of bootstrap statistics guarantees that $f_{\rm boot}(Q_4)$ tends to the desired distribution of $f(Q_4)$ in the limit of large $N_{\rm boot}$ and $N_{\rm sim}$. In practice, we used $N_{\rm boot}$ = 3000, $N_{\rm sim}$ = 2000, and $N_{\rm real}$ = 129 and then estimated $P_{\rm fit}$ as $F_{\rm boot}(Q_4^{\rm real})$. If $P_{\rm fit}$ is small, we can reject the corresponding model with confidence $1 - P_{\rm fit}$.

3. Updated models for pulsars in the region surrounding the Sun

To disentangle the effects that new pulsar distances, electron density model and velocity distribution have on our simulations, we first implement these changes one by one. All simulations in this section, unless stated otherwise, have the same parameters as those in Paper I: orbits are calculated only perpendicular to the galactic plane, the positions of pulsars projected on the galactic plane are drawn from a uniform distribution in a circle centered on the Sun with a radius of 3 kpc, the dispersion measure is calculated using Paper I's Eq. 16 and the velocity distribution is taken to be Gaussian in one dimension with a width of 110 km/s. Also, we use the same list of observed pulsars as in Paper I.

3.1. Luminosity distribution

Starting from the best models found in Paper I for assumed decay time scales of the magnetic field of 10 and 100 Myr, we have calculated a series of models on a grid of a and b values (see Eq. 3 and Fig. 2) in the ranges $0.6<a<2.4$ and $2.6<b<4.8$, keeping all other parameters fixed. We find that this does not improve significantly on the results for the KS-test in our simulations.

For the 100 Myr decay time, this can be understood since the KS tests from Paper I can hardly be improved upon. For the 10 Myr decay time, the problem was and remains that it is not possible to simultaneously fit the period distribution and the magnetic field distribution, while also having good fits to the dispersion measure and luminosity. By reducing the value of b, i.e. widening the luminosity distribution, one can fit the distributions of both the pulse periods and magnetic fields, but this leads to simulated distributions with unacceptably high dispersion measures and luminosities, as too many distant pulsars are detected.

3.2. Dispersion measure

Implementation of the Taylor and Cordes model for the electron density leads to an increase in distance of many nearby radio pulsars, and thus decreases the number of real pulsars with $d_{\rm proj} < 3$ kpc from 130 to 113 pulsars. It also means that the luminosities of the real pulsars we test against are higher, as illustrated in Fig. 3. Thus, if we keep the same luminosity laws as in Paper I, we find that the simulations both at 100 Myr and 10 Myr decay times lead to simulated luminosities that are too low. By adapting a to the lower value of 1.4, we can bring the simulated luminosities into agreement with the (newly determined) luminosities of the real pulsars. Surprisingly, the dispersion measures are now (slightly) less well fit than with the old model, and thus the overall fit to the observations is (slightly) worse.

If one also reduces b, the 10 Myr case improves significantly and becomes just as good as the 100 Myr case. As discussed in Sect. 3.1 a low value of b, while producing good fits to the period and magnetic field distributions, produced pulsars with higher

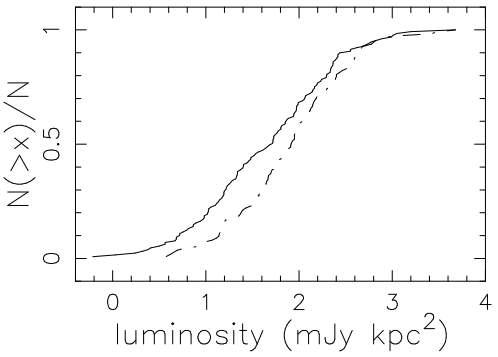

Fig. 3. The cumulative luminosity distribution of real pulsars with $d_{\rm proj} < 3$ kpc derived using the model for the galactic electron distribution of Paper I (solid line), and using the Taylor & Cordes (1993) model (dash-dotted).

luminosities and dispersion measures than the real pulsars in the old dispersion model. The new dispersion model, however, reduces the dispersion measure of simulated high-z pulsars, and increases the luminosities of the real pulsars, leading to good fits for all four quantities used in the Kolmogorov-Smirnov tests.

3.3. Velocity distribution

The Lyne & Lorimer velocity distribution has a higher root-mean-square velocity than the Gaussian distribution with σ_v = 110 km/s that we used in most models of Paper I.

Implementing this velocity distribution, but keeping the old model for the electron density distribution, we find a simulated population with too many pulsars at short pulse periods, just as in our simulation in Paper I with an increased root-mean-square velocity of 220 km/s: old, spundown pulsars have moved too far to be detected. This is worse for the simulation with short decay time, because field decay increases the time required to spin down to long periods.

The larger velocities, as modelled by Lyne & Lorimer (1994) are mainly the result of higher distances implied by the Taylor & Cordes model for the electron density. When we implement the Lyne & Lorimer velocity distribution together with the new electron density model, and further take a lower value for a, the 100 Myr simulations fit the observations acceptably: old pulsars have moved further out, but are detected due their higher luminosities. This does not hold for the 10 Myr simulations, since, as in Sect. 3.1, it is not possible to simultaneously fit the period distribution and the magnetic field distribution, while also having good fits to the dispersion measure and luminosity.

4. Pulsars in the galaxy

We now turn to the models in which all modifications have been implemented. The input distributions and parameters used in our simulations of pulsars moving in the whole galaxy are summarized in Table 2.

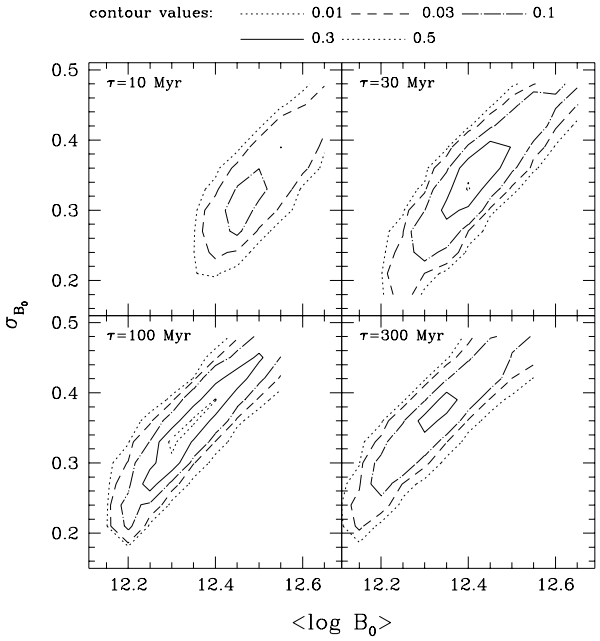

Fig. 4. Contours of equal probability $P_{\rm fit}$ on a grid of the mean and the width of the initial magnetic field distribution, for Model $\rm A_{\it B}$.

4.1. Models with standard parameters

The simulations which we will discuss first, are those of models A, $\rm A_{\it B}$, $\rm A_{\it L}$ in Table 2. In these models, the distribution of the birthplaces of neutron stars in our Galaxy is an exponential function of the distance to the galactic center, with scale length 5 kpc, and an exponential function of distance to the galactic plane, with scale height 60 pc. The neutron stars are born with an initial period of 0.1 s, and with a distribution of magnetic fields which is a Gaussian in log B. The velocities of the newly born pulsars are drawn from the distribution derived by Lyne and Lorimer (1994). Once the neutron stars have evolved to their current position, pulse period, and magnetic field strength, we determine whether they are above the death-line, and whether their beam crosses the Earth, where the beaming is described as in Vivekanand and Narayan (1981). We keep only pulsars with $d_{\rm proj} < 4$ kpc. If these conditions are met, the luminosity is determined from the equation given by Prószyński and Przybicień (1984), with a spread around this according to the description by Narayan and Ostriker (1990). We then test whether the simulated pulsar is detectable by any of four surveys, and if so, add it to the list of simulated detections. This procedure is continued until 2000 pulsars in the simulation are detected, after which their properties are compared to those of the real pulsars detected in the same four surveys.

In Model $\rm A_{\it B}$, we vary the center and width of the distribution of initial magnetic field strengths, and in Model $\rm A_{\it L}$ we vary the center and width of the distribution of luminosities around the value given by the luminosity law.

In Fig. 4 we show for which combinations of the central value log B_o and width σ_B of the Gaussian distribution of initial

Table 2. Equations and parameters used in the simulations discussed in Sect. 4. An equation number preceded by I refers to an equation in Paper I.

pulsar property	chosen distribution	equation number	parameter value
	Model A		
initial position in Galaxy	exponential in galactocentric distance R	Eq. 4	$R_{\rm w}$ = 5 kpc
	exponential in distance to Galactic Plane	Eq. I7	h = 60 pc
initial velocity	Lyne-Lorimer distribution		
initial pulse period			$P_{\rm i}$ = 0.1 s
initial field strength	Gaussian in log B	Eq. I1	log B_o = 12.32, σ_B = 0.34
field decay	exponential	Eq. I3	τ = 10 − 300 Myr
beaming	Vivekanand & Narayan	Eq. I5	
death line		Eq. I13	
electron distribution model	Taylor & Cordes		
maximum distance projected on Galactic Plane ($d_{\rm proj}$)			4 kpc
luminosity	luminosity law	Eq. 2	
	spread around law value	Eq. 3	a = 1.5, b = 3.5
	Model B, as A except		
initial velocity	Phinney-Paczyński distribution	Eq. 1	σ_v = 600 km/s
	Model C, as A except		
initial position in Galaxy	Gaussian	Eq. 5	$R_{\rm w}$ = 4.8 kpc , $R_{\rm off}$ = 0
	Model D, as A except		
initial position in Galaxy	offset Gaussian	Eq. 5	$R_{\rm w}$ = 1.8 kpc , $R_{\rm off}$ = 3.5 kpc
	Model X$_B$, as X(∈ A,B,...) except		
initial field strength	Gaussian in log B	Eq. I1	$12.15 < \log B_o < 12.65$, $0.18 < \sigma_B < 0.48$
	Model X$_L$, as X(∈ A,B,...) except		
luminosity	spread around law value	Eq. 3	$0.6 < a < 2.4$, $2.6 < b < 4.8$

magnetic field strengths the best descriptions of the data are obtained, for decay times ranging from 10 Myr to 300 Myr. The quality of the fit is determined by Kolmogorov-Smirnov tests comparing the simulated and real distributions of the pulsar properties P, B, DM sin b and L_{400}, as explained in Sect. 2.6. We have verified that the region in the log B_o vs. σ_B plane where the best solutions are found is the same for different choices of pulsar properties on which the tests are performed.

As in Paper I, we see that the models with long decay times give a significantly better description of the observations: the shortest decay time of 10 Myr can be rejected with 85% confidence, and decay times of 30 Myr and more give acceptable fits to the data. Since the values of $P_{\rm fit}$ reach to above 50%, we can also conclude that our best models are good enough in an absolute sense, i.e. their fit quality is not less than what could be expected of a perfect model. Given all the imperfections like the uncertain luminosity distribution and the undoubtedly imperfect model for the electron density in the Galaxy, this may be a bit of a surprise. As in Paper I, we find that there is a correlation between the values of log B_o and σ_B for good fits: to model a sufficient number of pulsars with weak magnetic fields, the model with high average field strength must have a wide distribution around it. In the calculations for Fig. 4 we chose the values a = 1.5 and b = 3.5 for the parameters describing the luminosity spread (see Eq. 3), to take into account the effect of a new distance scale on the observed luminosity distribution discussed in Sect. 3.

In Fig. 5 we illustrate the region in the a vs. b plane where the best solutions are found. This region depends little on the chosen values of the distribution of initial magnetic field strengths, in the range where the best solutions are found. The region is also similar for short and long decay times. We see that there is an anticorrelation between the best values of a and b, which means that a large value for a, i.e. a low minimum luminosity, requires a low value of b, i.e. a large spread in luminosities, in order to obtain a sufficient number of luminous pulsars.

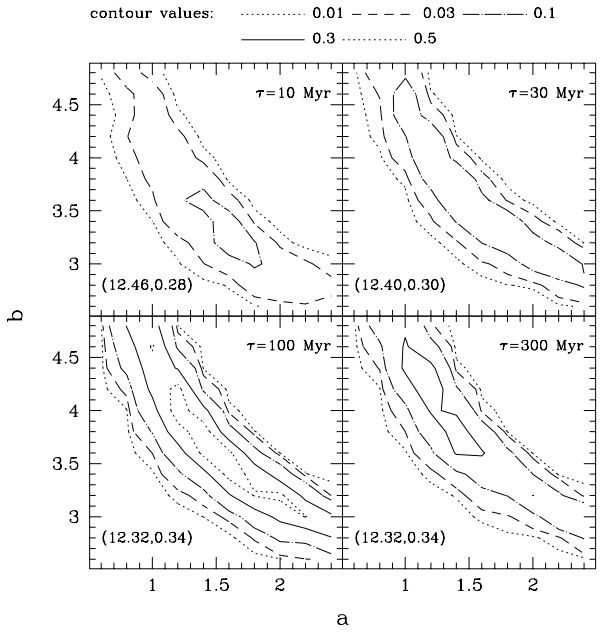

Fig. 5. Contours of equal probability $P_{\rm fit}$ on a grid of the shift a and width b of the luminosities $\log L_{400}$ around $\log L_{\rm m}$, for Model A_L. Each panel is labelled with its decay time in the top right and the combination of $(\log B_0, \sigma_{B_0})$ used at the bottom. These latter combinations were chosen to be near the maximum probability in the corresponding panel in Fig. 4.

4.1.1. The best models with long decay times

The selection effects that operate in the observations of radio pulsars strongly favor the detection of pulsars relatively close to the Sun. In order to be detectable at all, pulsars must be beamed towards the Earth, and above the death line. (As explained in Paper I, such pulsars are younger on average than the overall neutron star population. See also Fig. 7 below.) Selecting such well-beamed simulated pulsars above the death line, but before checking whether they are actually detected in the simulated surveys, we find that 23% of the pulsars currently at $d_{\rm proj} < 4\,$kpc were born at $d_{\rm proj} < 4\,$kpc. However, if we subsequently select the pulsars that are also detected, we find that 56% of these were born at $d_{\rm proj} < 4\,$kpc, even though a second peak is still visible for initial positions close to the Galactic Center. Overall, the concentration of detected radio pulsars towards the Galactic Center is much smaller than for the birth place distribution given by Eq. 4. This is illustrated in Fig. 6.

Note that $d_{\rm proj}$ is defined to the current position of the Sun. Since many pulsars are young compared to the rotation period of the Sun around the Galactic Center, the percentages just given provide a rough indication of the fraction of pulsars now close to the Sun which were also close to the Sun when they were born. If we take the motion of the Sun into account, we find that 62% of the pulsars detected in Model A were born at a distance projected on the Galactic Plane of less than 4 kpc to the position of the Sun at the time of pulsar birth.

The velocities of neutron stars are high, generally, compared to those of ordinary stars in the Galaxy, and consequently, old neutron stars are spread over a much larger volume in the Galaxy than young neutron stars. In the area around the Sun, the number density of old neutron stars is therefore low, compared to that of younger neutron stars. This kinematic selection of young neutron stars is added to the selections effected by the demand that the pulsar must be beamed towards the Earth and above the death-line, as illustrated in Fig. 7.

(No such kinematic selection operated in our Paper I, where the motion of pulsars was limited to the direction perpendicular to the Galactic Plane.) The high velocities of the pulsars also lead to an increased distance of detectable pulsars from the Galactic Plane, also illustrated in Fig. 7.

Because of the correlations between youth and luminosity of a pulsar, and between proximity and flux, the detected pulsars in our simulations are young and generally close to the Galactic Plane, which tends to mask the kinematic effects on the age and z-distributions of the pulsars.

The best models with long decay times fit the period, magnetic-field strength, luminosity, and age distributions rather well, but do less well in fitting the distribution of dispersion measures (or $DM \sin b$), as illustrated in Fig. 8. The problem in fitting the dispersion measure is all the more remarkable, as our new simulations use a more elaborate model for it. The best models also do less well in fitting the flux distribution, which is remarkable since both the luminosity and the distance distributions are well fitted. We return to the dispersion measures and the fluxes in Sect. 5.

The galactic birth rate of radio pulsars in Model A is about 1 per 290 years.

4.1.2. The failure of models with short decay times

Models with short decay times cannot simultaneously reproduce the distributions of the pulse periods and the magnetic fields, for models which fit the luminosity distribution well. The reason for this is that the rapid field decay allows pulsars to reach long periods only if their initial field strength is very high. A model that fits the observed distribution of field strengths has too few pulsars at long periods, whereas a model with the observed period distribution has too many pulsars with high magnetic fields. One can try to remedy this by biasing the selection effects towards longer periods. This can be done by shifting the luminosity distribution towards higher luminosities, via a reduction in the value of a, as most less luminous pulsars thus brought above the detection limit have long periods (see Fig. 2). Thus, for $a = 0.60$ a model can be constructed with a decay time of 10 Myr that correctly reproduces both the pulse period and the magnetic field strength distributions, but only at the cost of predicting far too many luminous pulsars. This is illustrated in Fig. 9. These high luminosities also allow too many pulsars in the simulations to be detected at large distances from the Sun.

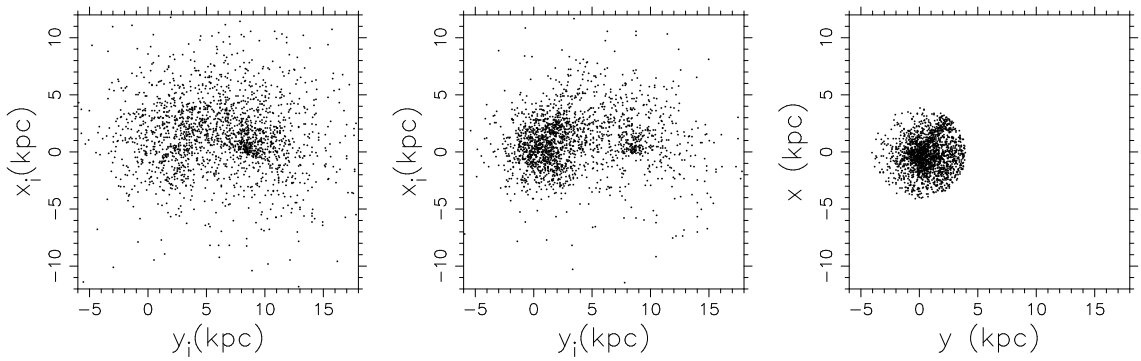

Fig. 6. Positions in the Galaxy for pulsars in Model A, with a decay time of 100 Myr. The left frame shows the birthplaces in the Galaxy of pulsars with $d_{\rm proj} < 4$ kpc, and which are above the death line and beamed towards the Earth. The middle frame shows the birthplaces in the Galaxy for pulsars detected in our simulation, and the right frame the current position of these pulsars. Notice that the coordinate frame used in this picture is fixed, i.e. does not corotate with the Sun.

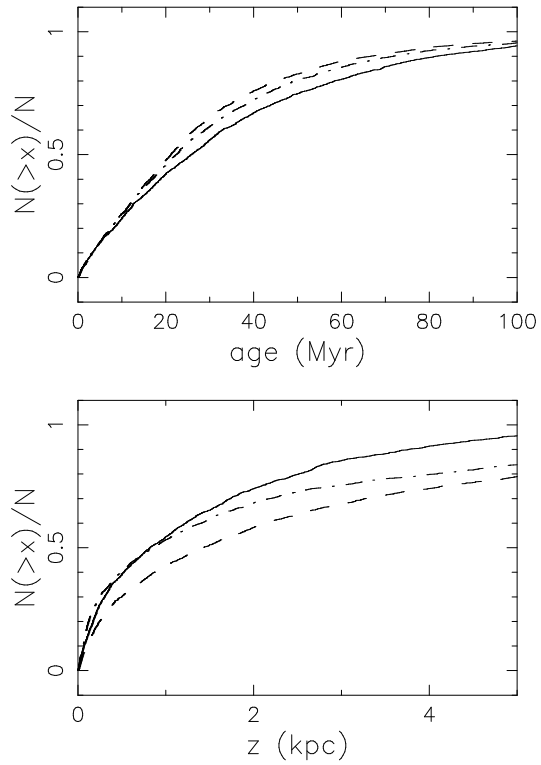

Fig. 7. Cumulative age (top panel) and z (bottom panel) distributions for pulsars beamed towards Earth and above the deathline, but not tested for detection, in simulations with τ = 100 Myr. Solid lines: according to Paper I, dashed lines: the pulsars with $d_{\rm proj} < 4$ kpc in Model A, dash-dotted lines: the pulsars with $d_{\rm proj} < 4$ kpc in Model B.

4.2. Variations on the input parameters

In varying the parameters of the models, we find that good fits to the observations can be found for different input assumptions. Thus, model B, in which the velocity distribution of pulsars at birth is described by Eq. 1, gives results which are very similar to those of model A. Model $\rm B_B$ and Model $\rm B_L$ produce good fits of the observations for very similar values of $\log B_o$, σ_B, a and b as models $\rm A_B$ and $\rm A_L$ for a decay time of 100 Myr, and they cannot produce acceptable fits for a decay time of 10 Myr. In model B a somewhat larger fraction of the radio pulsars detected in the simulations were born at galactocentric radii in the range $4.5 - 12.5$ kpc than in model A, in which more pulsars have sufficiently high velocities to enter this range from either smaller or larger galactocentric radii. Thus, 69% of all pulsars detected in Model B was born at a distance projected on the Galactic Plane of less than 4 kpc to the position of the Sun at the time of pulsar birth.

Model B gives a somewhat better description than model A of the correlation between characteristic age τ_c and distance to the Galactic Plane z, in the sense that the models with higher velocities produce too many pulsars with small characteristic age at large distances from the Plane. We compare the real and simulated pulsars with a two-dimensional Kolmogorov-Smirnov test, as follows (see Press et al. 1992, chapter 14.7). The position of a simulated detected pulsar in the τ_c-z plane defines four quadrants: upper left, upper right, lower left, lower right. We determine the fraction of simulated pulsars and the fraction of real pulsars, and the difference between them, in each quadrant, and keep the highest difference d_f. The distribution of d_f found for the positions of all simulated detections may be used to estimate the probability that both distributions are the same. For Model B the difference d_f is larger than 10% in only very few points, and the probability that real and simulated distributions are the same is 29%, in a calculation with 10^4 simulated detections. In contrast, the difference d_f is larger than 10% in rather more points in Model A, and the probability that real and simulated distributions are the same is only 5%, again in a calculation with 10^4 simulated detections. The positions of large d_f in this model are concentrated at small characteristic age and large $|z|$, as illustrated in Fig. 10.

Since many pulsars detected in the simulations were born relatively close to the (then) position of the Sun, we suspect that our simulations do not probe the birth rate of radio pulsars at small galactocentric radii very well. To investigate this, we

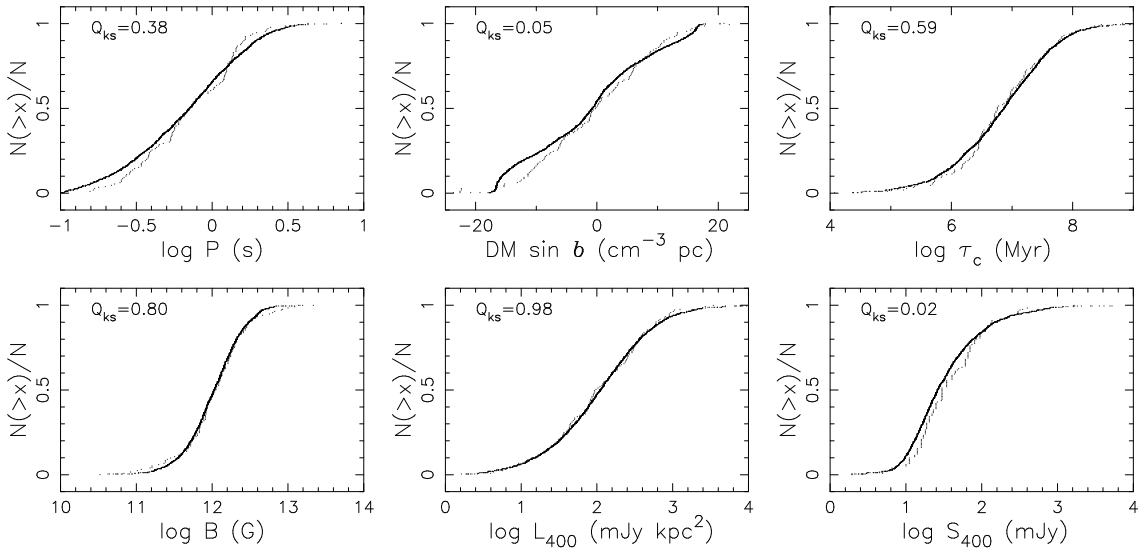

Fig. 8. Cumulative distributions of real pulsars (dots) and of pulsars from Model A, with a decay time of 100 Myr. The probability, according to a Kolmogorov-Smirnov test, that the real and simulated distributions are drawn from the same distribution is indicated in each frame.

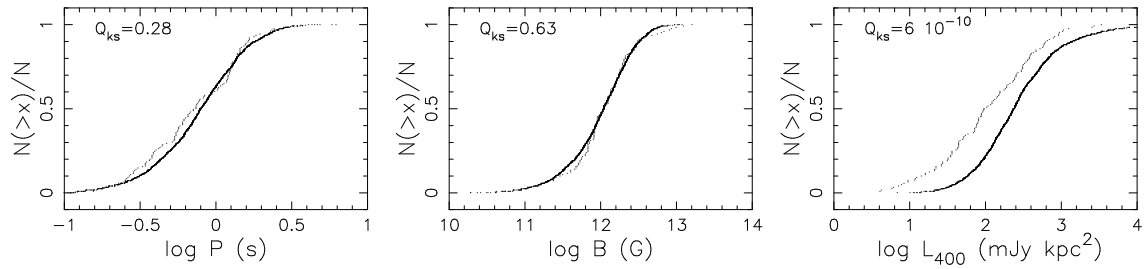

Fig. 9. Cumulative distributions of real pulsars (dots) and of pulsars from a simulation with a decay time of 10 Myr, illustrating that the distributions of pulse periods and of magnetic field strengths can be described in a model with a short decay time, only when the simulated pulsars have unnacceptably high luminosities. The model illustrated uses a = 0.60, b = 3.4 in Eq. 3, and has log B_o = 12.46 and σ_B = 0.28.

calculated a model, identical to Model A except for the fact that the pulsar birth rate was taken zero at galactocentric radii less than 2 kpc. This model describes the observations as well as Model A, and in fact fits the $DM \sin b$ distribution marginally better. The galactic birth rate of neutron stars in this model is 1 per 430 years. In Model C the birth rate of pulsars has a Gaussian distribution in galactocentric radius. The most important difference for our calculations between this model and Model A is the slope of the gradient in the birth rate function near the Sun. Again, this model gives a good description of the data. Apparently, what matters in the birth rate function is that sufficient number of pulsars are born locally, rather than the exact shape of the birth rate function (see also Model D below). In Model C the $DM \sin b$ distribution is fitted marginally better than in Model A (with $Q_{ks}(DM \sin b)$ = 0.14). The galactic birth rate of neutron stars in this model is 1 per 315 years.

We also investigate a model in which very few pulsars are formed near the Sun, so that pulsars now found near the Sun have migrated from smaller galactocentric radii. With an eye on the electron density in the Galactic Plane from the model by Taylor & Cordes (1993), we choose for model D $R_{\rm off}$ = 3.5 kpc and $R_{\rm w}$ = 1.8 kpc in Eq. 5. (Thus the spiral arms are not included.) We find that this model produces too few pulsars at short periods, and contains far too many old pulsars ($Q_{ks}(\log P)$ = 0.04, $Q_{ks}(\log \tau_c)$ = 0.0005): because relatively few pulsars are born near the Sun in this model, the pulsars detected near the Sun have slowed down and aged a lot while migrating from the smaller galactocentric radii where they were born.

5. Discussion

5.1. Birth rate and progenitor mass

The comparison between observation and simulation in our calculations is done in the region surrounding the Sun, with $d_{\rm proj} < 4$ kpc. Because a large fraction of the locally observed pulsars were also produced locally (see the discussion of Fig. 6), our calculations constrain the formation rates of neutron stars near the Sun, but they cannot discriminate between models that have rather different formation rates elsewhere in the Galaxy. As discussed in Sect. 4.2, a modification of Model A in which

the neutron star birth rate is equal to zero at galactocentric radii $R < 2$ kpc, gives as good a description of the observations as model A itself. Similarly, models A and C, with their very different galactocentric distributions of neutron star birth rates, both give adequate descriptions of the observations. Our models therefore do not constrain the galactic supernova rate very strongly.

From the Galactic birth rate of neutron stars of about 3400 per Myr in Model A, we derive (through Eq. 4) a birthrate near the Sun of about 2.3 kpc^{-2}Myr^{-1}. Blaauw (1985) estimated that OB associations near the Sun produce neutron stars at a rate of about 3 kpc^{-2}Myr^{-1}. Using this number, we find that the local production of neutron stars according to Model A may be adequately explained with a formation in the OB associations only, if we assume constant birthrates during the characteristic ages of the radio pulsars.

Blaauw himself came to the opposite conclusion, viz. that most neutron stars near the Sun are produced from less massive B stars, away from the associations. The reason for his conclusion was his much higher estimate for the birth rate of neutron stars near the Sun: the pulsar catalogue of Manchester & Taylor (1981) contains 26 pulsars at $d_{\rm proj} < 0.5$ kpc, and Blaauw assumed that all of these must have been produced during the last 4.6 Myr, in accordance with the then current view that rapid field decay limits the time span during which pulsars are detectable. With a beaming factor of about 3, this gives a birth rate of neutron stars of about 20 kpc^{-2}Myr^{-1}. The main reason for the much lower birth rate in our Model A is the much longer time interval that it allows for the production of the locally detected pulsars.

We can illustrate this with a new look at the locally detected pulsars. The catalogue by Taylor et al. (1993) contains 33 pulsars at $d_{\rm proj} < 0.5$ kpc; 9 are recycled pulsars in binaries, and 2 more (with unknown period derivative) are almost certainly recycled, with periods of 0.0049 and 0.0052 s. Thus, there are about 22 ordinary (in the sense of not recycled) pulsars at $d_{\rm proj} < 0.5$ kpc, of which 17 with known $\dot{P}$. 2 pulsars of the 17 with known $\dot{P}$ are younger than 4.6 Myr, and the median age of these 17 pulsars is about 17 Myr. The number 22 of locally detected ordinary pulsars is similar to the number of 26 used by Blaauw (1985), but from their age distribution we derive that only 2 or 3 of these 22 were produced in the last 4.6 Myr.

Again using an average beaming factor of 3, we note from Table 3 of Blaauw (1985) that progenitors with masses in excess of $\sim 10\ M_\odot$ can produce a sufficient number of neutron stars to account for the observed population. This value for the progenitor mass is in agreement with the derivation by Koester & Reimers (1988), from the detection of white dwarfs in the open cluster NGC2451, that stars with masses up to $\sim 8\ M_\odot$ may still produce white dwarfs.

Ramachandran & Deshpande (1994) have found a correlation between the current positions of the detected radio pulsars and the position 60 Myr ago of the galactic spiral arms, and explain this assuming a) that the typical progenitor of a neutron stars is a B star which lives for 50 Myr before exploding as a supernova, b) that the typical age of the detected radio pulsars is 10 Myr, and c) that pulsars haven't moved far during their life. According to the discussion in the previous paragraphs, most neutron star progenitors may in fact be O or B stars in OB associations; these stars have life times less than 30 Myr. We have also seen that the ages of detected radio pulsars has a very wide spread, and extend to much longer than 10 Myr. Therefore, we see no reason for a correlation peaked on 60 Myr. In addition, in Model A the median of the product of the initial peculiar velocity and the age of the detected pulsars is 2 kpc, larger than half the distance between different spiral arms at the solar galactocentric radius.

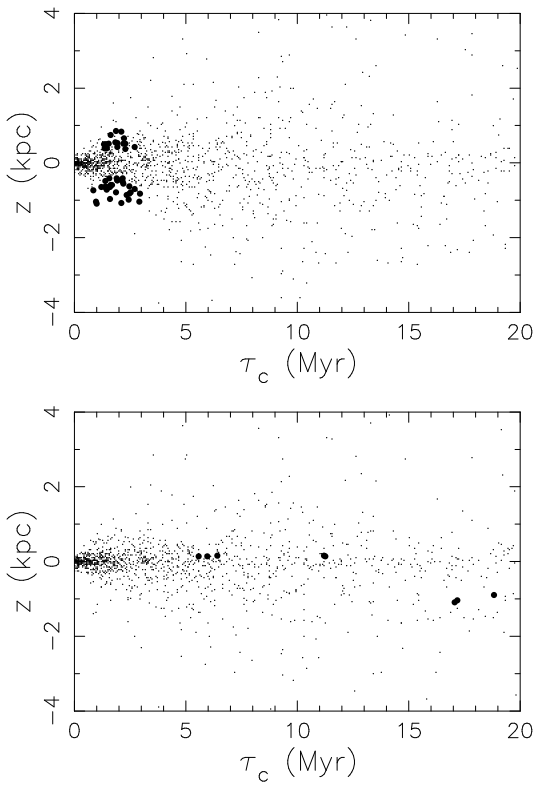

Fig. 10. The distribution of simulated pulsars in the τ_c-z plane for Model A (above) and for Model B (below). The simulated pulsars for which d_f is larger than 10% are shown with larger symbols.

5.2. Distance to galactic plane

In models with a long decay time, pulsars with a large characteristic age are old enough to have experienced appreciable deceleration by the galactic potential (Hartman & Verbunt 1995). Lorimer (1994, 1996) points out that such models predict a decrease of the average distance to the plane at the highest observed characteristic ages, with respect to the average distance at intermediate characteristic age, in agreement with the observations. We confirm this result, as may be seen in Fig. 11. Also in agreement with Lorimer (1994), we find that the model predictions for the average distance to the plane are slightly above the observed values. The predicted average distance to the plane is smaller in Model B, in which a larger fraction of the pulsars are born at

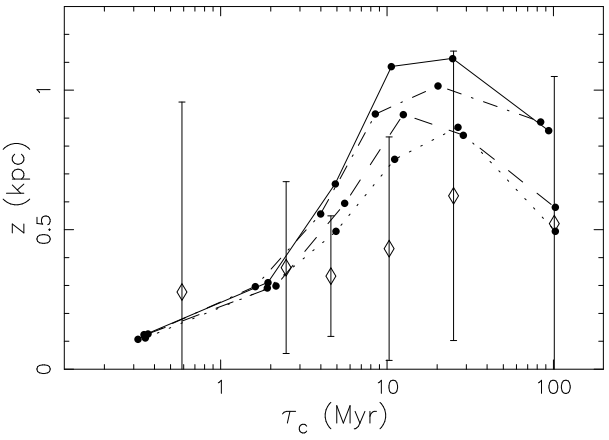

Fig. 11. Average distance to the galactic plane for the real pulsars in our comparison sample, as derived from the Taylor & Cordes (1993) model for the galactic electron distribution (◇), and as predicted in Model A (solid line), Model B (dashed line), and in variants of these models in which the birth rate of neutron stars is zero at galactocentric radii $R < 2$ kpc (dash-dotted and dotted, respectively for variants on A and B).

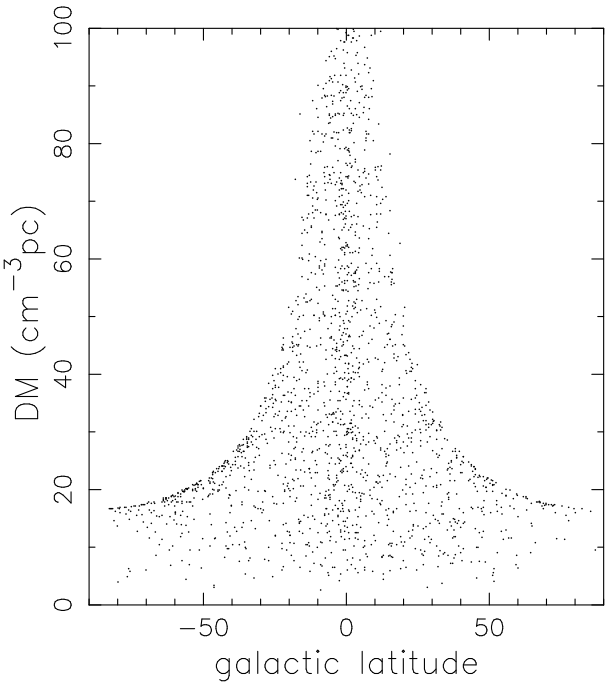

Fig. 12. The galactic longitude vs dispersion measure for Model A. A two-dimensional KS test gives a probability of 24% that this distribution is consistent with the observed distribution.

small velocities. The predicted average distance to the plane is also somewhat smaller in models in which the birth rate of neutron stars peaks less towards the galactic center than in Model A, such as in our variant of Model A in which the birth rate is zero at galactocentric radii $R_i < 2$ kpc and in our Model D. The models predicting smaller average distances give a slightly better description of the observed distribution of $DM \sin b$.

The high average distances to the galactic plane of the pulsars in our models is a direct consequence of the large average birth velocity of pulsars, and accordingly, a relatively large number of pulsars have dispersion measures near or at the maximum in each direction due to the limit to the vertical extent of the electron layer near the Sun (see Fig. 12). We speculate that the fraction of neutron stars that is born with small velocities is somewhat larger than in our models, or alternatively that the vertical scale height of the galactic electron distribution is somewhat larger than according to the description by Taylor & Cordes (1993).

The cumulative flux distribution in our models is shifted by about 25% with respect to the observed flux distribution, as may be seen from Fig. 8 for the case of Model A. We think that this is related to our modelling of the detections near the detection limit, which has a sharp transition between detectable and non-detectable flux, whereas the transition in real observations will be more gradual, especially if we take into account that pulsar fluxes can vary due to interstellar scintillation. We have investigated this by adding the constraint that the pulsar flux must be in excess of 10 mJy to the flux detection limits as described in Paper I. The sample of real pulsars is slightly reduced from 129 pulsars to 123 pulsars by this extra constraint, but the simulated flux distribution in Model A is shifted sufficiently to give a good description of the distribution of $\log S$ of these 123 real pulsars. We therefore think that the differences between simulated and observed flux distributions for our best models are indeed due to our necessarily rough description of the detection limits, and that these differences do not invalidate our conclusion that these models give good descriptions of the observations.

5.3. Models for the whole galaxy

In the models described so far simulation of the observations was limited to $d_{\rm proj} < 4$ kpc, both because the model for the electron density is more reliable near the Sun, and because the use of interpolations in a grid for the dispersion measures (as described in Sect. 2.1) allows us to considerably reduce the computational cost. The question arises how well the best models describe the observations at larger distances. We have done a few calculations to investigate this, in which we simulate observations out to $d_{\rm proj} = 10$ kpc. The comparison sample of real pulsars increases to 206 pulsars. Model A, modified to have $d_{\rm proj} = 10$ kpc, produces too many high luminosity pulsars. We amend this by decreasing the width of the luminosity distribution, setting $b = 3.85$, and find that this produces good fits to the distributions of $\log B$, $\log L$ and $\log \tau_c$, and marginally acceptable fits to $\log P$ and $DM \sin b$. The problems with the latter two are the same as visible in the simulations with $d_{\rm proj} < 4$ kpc, shown in Fig. 8, made more significant by the larger comparison sample, viz. the simulated period distribution is too broad, and too many pulsars have high absolute values of $DM \sin b$. Also, the characteristic ages of the simulated pulsars are too high.

The larger width of the period distribution in our simulations suggests a slightly inaccurate description of the period depen-

dence of selection effects, e.g. in our modelling of the beaming factor, or of the luminosity. We think that the fit to the dispersion measures could be improved by adding random fluctuations to the dispersion model by Taylor & Cordes (1993), thus taking into account the inhomogeneity of the electron distribution: this will reduce the excess of simulated pulsars at the maximum $DM \sin b$ visible at $|DM \sin b| \simeq 15$ cm^{-3} pc in Fig. 8 (see also Fig. 12). Nelemans et al. (1997) model the variance in dispersion measure and implement it in our population synthesis.

We have also calculated Model A out to $d_{\rm proj} = 10$ kpc for a decay time of 10 Myr and find that this describes the observations very well! This is due to the shift of the luminosity distribution of the observed pulsars towards higher luminosities when $d_{\rm proj}$ is increased from 4 to 10 kpc (see also the discussion in Sect. 4.1.2). We intend to study models in which observations are simulated for the whole Galaxy in more detail. Before doing so, we are hesitant to draw inferences from our preliminary results in view of the uncertainties in distance determination and in our knowledge of the spatial distribution of pulsar birth places at large distances from the Sun.

Similar conclusions can be drawn from our application of Model B to $d_{\rm proj} < 10$ kpc. On the whole we consider the success of the best models in describing the pulsar population of a much larger part of the Galaxy to be very encouraging.

References

Bhattacharya, D. 1995, JA&A, 16, 217

Bhattacharya, D., Verbunt, F. 1991, A&A, 242, 128

Bhattacharya, D., Wijers, R., Hartman, J., Verbunt, F. 1992, A&A, 254, 198

Blaauw, A. 1985, in W. Boland, H. van Woerden (eds.), Birth and Evolution of Massive Stars and Stellar Groups, Reidel, Dordrecht, p. 211

Carlberg, R., Innanen, K. 1987, ApJ, 94, 666

Damashek, M., Taylor, J., Hulse, R. 1978, ApJ, 225, L31

Davies, J., Lyne, A., Seiradakis, J. 1972, Nat, 240, 229

Deshpande, A., Ramachandran, R., Srinivasan, G. 1995, JA&A, 16, 53

Hartman, J., Verbunt, F. 1995, A&A, 296, 110

Hulse, R., Taylor, J. 1974, ApJ, 191, L59

Johnston, S. 1994, MNRAS, 268, 595

Koester, D., Reimers, D. 1988, A&A, 153, 260

Kuijken, K., Gilmore, G. 1989, MNRAS, 239, 571,605

Lorimer, D. 1994, *Ph.D. thesis*, University of Manchester

Lorimer, D. 1996, in S. Johnston, M. Walker, M. Bailes (eds.), Pulsars, problems and progress. IAU Coll.160, p.31

Lorimer, D., Bailes, M., Dewey, R., Harrison, P. 1993, MNRAS, 263, 403

Lyne, A., Lorimer, D. 1994, Nat, 369, 127

Manchester, R., Lyne, A., Taylor, J., Durdin, J., Large, M., Little, A. 1978, MNRAS, 185, 409

Manchester, R., Taylor, J. 1981, AJ, 86, 1953

Narayan, R., Ostriker, J. 1990, ApJ, 352, 222

Nelemans, G., Hartman, J., Verbunt, F., Bhattacharya, D., Wijers, R. 1997, A&A, in press

Paczyński, B. 1990, ApJ, 348, 485

Phinney, E., Blandford, R. 1981, MNRAS, 194, 137

Press, W., Flannery, B., Teukolsky, S., Vetterling, W. 1992, Numerical Recipes: The Art of Scientific Computing 2nd ed., Cambridge U. P., Cambridge

Prószyński, M., Przybicień, D. 1984, in S. Reynolds, D. Stinebring (eds.), Millisecond Pulsars, NRAO, Green Bank, p. 151

Ramachandran, R., Deshpande, A. A. 1994, JA&A, 15, 69

Reynolds, R. 1989, AJ, 339, L29

Taylor, J., Cordes, J. 1993, ApJ, 411, 674

Taylor, J., Manchester, R., Lyne, A. 1993, ApJS, 88, 529

Verbunt, F. 1994, in S. Holt, C. Day (eds.), The Evolution of X-ray Binaries, AIP, New York

Vivekanand, M., Narayan, R. 1981, JA&A, 2, 315

This article was processed by the author using Springer-Verlag LaTeX A&A style file *L-AA* version 3.